Title

Absolute cerebral blood flow: Assessment with a novel low-radiation-dose dynamic CT perfusion technique in a swine model

Journal

Journal of Neuroradiology, 49(2)

ISSN

0150-9861

Authors

Abbona, Pablo
Zhao, Yixiao
Hubbard, Logan
et al.

Publication Date

2022-03-01

DOI

10.1016/j.neurad.2021.09.003

Peer reviewed

HHS Public Access

Author manuscript

J Neuroradiol. Author manuscript; available in PMC 2022 June 24.

Published in final edited form as:

J Neuroradiol. 2022 March ; 49(2): 173–179. doi:10.1016/j.neurad.2021.09.003.

Absolute cerebral blood flow assessment with a novel low-dose dynamic CT perfusion technique in a swine model

Pablo Abbona, MD[a],

Yixiao Zhao, MS[a],

Logan Hubbard, Ph.D[a],

Shant Malkasian, BS[a],

Brooklynn Flynn, BS[a],

Sabee Molloi, Ph.D.[a]

[a]Department of Radiological Sciences, University of California, Irvine, Irvine, California, 92697, USA

Abstract

Rationale and Objectives: To validate the accuracy of a novel low-dose dynamic CT perfusion technique in a swine model using fluorescent microsphere measurement as the reference standard.

Materials and Methods: Contrast-enhanced dynamic CT perfusion was performed in five swine at baseline and following brain embolization. Reference microspheres and intravenous contrast (370 mg/ml iodine, 1 ml/kg) were injected (5 ml/s), followed by dynamic CT perfusion. Scan parameters were 320×0.5 mm, 100 kVp and 200 mA. On average, 47 contrast-enhanced volume scans were acquired per acquisition to capture the time attenuation curve. For each acquisition, only two systematically selected volume scans were used to quantify brain perfusion with first-pass analysis technique. The first volume scan was selected at the base, simulating bolus tracking, while the second volume at the peak of the time attenuation curve similar to a CT angiogram. Regional low-dose CT perfusion measurements were compared to the microsphere perfusion measurements with t-test, linear regression and Bland-Altman analysis. The radiation dose of the two-volume CT perfusion technique was determined.

Results: Low-dose CT perfusion measurements (P_{CT}) showed excellent correlation with reference microsphere perfusion measurements (P_{MICRO}) by $P_{CT} = 1.15\ P_{MICRO} - 0.01$ ($r = 0.93$, $p \leq 0.01$). The CT dose index and dose-length product for the two-volume CT perfusion technique were 25.6 mGy and 409.6 mGy, respectively.

Conclusions: The accuracy and repeatability of a low-dose dynamic CT perfusion technique was validated in a swine model. This technique has the potential for accurate diagnosis and follow up of stroke and vasospasm.

Keywords

brain; stroke; perfusion; multidetector computed tomography; models; animal

Address for Correspondence: Professor Sabee Molloi, Ph.D., Department of Radiological Sciences, University of California, Irvine, Medical Sciences I, B-140, Irvine, CA 92697-5000, Phone: (949) 824-5904, symolloi@hs.uci.edu.

Introduction:

Stroke is a leading cause of mortality and disability. The incidence of acute ischemic stroke in the USA is about 800,000 patients per year (0.25% of the total population), and it is expected to increase significantly, due to the aging population[1]. Although there are challenges with the lack of standardization and accuracy of quantitative assessment, CT perfusion is evolving as a cornerstone for imaging-based strategies in the rapid management of acute ischemic stroke[2]. These challenges may be addressed with a low dose dynamic CT perfusion technique with currently available high temporal resolution CT scanners to image the whole brain in about 2 seconds. Characterizing the ratio of necrotic core to ischemic penumbral volume is fundamental for risk assessment and triage of ischemic stroke patients for intra-arterial thrombolytic intervention or medical treatment, where parameters such as cerebral blood volume, cerebral blood flow, and mean transit time are derived. Furthermore, dynamic CT perfusion techniques also are important in the evaluation of reperfusion and treatment response of patients with stroke[3], vasospasm in subarachnoid hemorrhage[4], and intracranial tumors[5].

Nevertheless, current conventional CT perfusion techniques suffer from a variety of problems such as variation in cerebral blood volume and cerebral blood flow measurements amongst different postprocessing algorithms[6 7], and high radiation dose (66-452 mGy)[8] secondary to the use of multiple scans over time to improve signal-to-noise ratio and measurement reliability. Hence, there is a major clinical need for an accurate, low-dose, dynamic CT perfusion technique for improved assessment of cerebral blood flow. The purpose of this study was to validate a new dynamic CT perfusion technique for low-dose absolute cerebral blood flow measurement as compared to reference standard fluorescent microsphere measurement in a swine model. The study assessed whether accurate and repeatable absolute cerebral blood flow measurement is feasible using only two optimally timed whole-brain volume scans and a single contrast injection.

Materials and Methods:

General Methods:

Five male Yorkshire swine (mean weight, 55 ± 24 kg) were used. The experimental protocol was approved by the Institutional Animal Care Committee and performed accordingly (AUP-18-191). In each animal, contrast-enhanced dynamic whole-brain CT scanning was performed at baseline and following multiple levels of incremental brain embolization. Each dynamic CT acquisition consisted of 40–50 consecutive volume scans over 30 seconds, in order to capture the entire arterial time-attenuation curve. Each time-attenuation curve was then used for systematic selection of two volume scans to calculate CT perfusion measurements which were validated versus reference standard fluorescent microspheres[9, 10] (Figures 1 and 2). Experimental data was prospectively acquired between April and October 2017 and were retrospectively analyzed between June 2018 and February 2019. All authors conducted the data acquisition. Y.Z., L.H., Sh.M., and B.F. conducted the data analysis, where Y.Z., L.H., Sh.M had three years of medical imaging research experience, while B.F.

had one. P.A., a radiologist with 15 years of clinical experience, also conducted the data analysis and the surgical and interventional procedures.

Animal Preparation:

Anesthesia was induced with Telazol (4.4 mg/kg) (Zoetis), Ketamine (2.2 mg/kg) (Vedco), and Xylazine (2.2 mg/kg), (Akorn). Endotracheal intubation was performed (6.0 – 8.0 mm) with the animal in supine position and general anesthesia was administered with 1.5–2.5% isoflurane (Baxter) in oxygen via mechanical ventilation (Surgivet and HME). Two femoral vein and four femoral artery vascular sheaths (Cordis) were placed under ultrasound guidance for intravenous contrast injection, drug and fluid administration, blood pressure monitoring, selective catheter brain embolization, reference fluorescent microsphere injection, and reference blood withdrawal, respectively. A catheter was placed in the ascending pharyngeal artery (equivalent to the internal carotid artery in humans) under fluoroscopic guidance for progressive embolization of the brain capillaries with microspheres (95 μm in diameter, 3M/Z-Light Spheres W-1000). Of note, in swine, the ascending pharyngeal artery terminates in the rete mirabile[11], an extensive arborization of small (250–700 μm) vessels that, after piercing the cavernous sinus dura, coalesce and form the internal carotid artery[12, 13]. The diameter of the embolization microspheres was smaller than the rete mirabile diameter, i.e., the microspheres passed freely through the rete mirabile, but larger than the average brain capillary diameter (4–7 μm), i.e., the microspheres resulted in progressive embolization of the brain. The animals were then euthanized, and their brains were surgically resected for reference fluorescent microsphere analysis.

Reference Fluorescent Microsphere Perfusion Measurement:

For each cerebral perfusion condition in each animal, 0.25 mL of fluorescent NuFLOW™ microspheres (15.5μm in diameter, IMT Laboratories) was diluted in 1.75 ml of saline injected into the heart left ventricle via a pigtail catheter, followed by dynamic CT acquisition. At the same time, a reference blood sample was withdrawn from the descending aorta at 10 ml/min using a syringe pump (GenieTouch; Kent Scientific), starting 5 seconds prior to fluorescent microsphere injection and lasting for 120 seconds. After each fluorescent microsphere injection and CT acquisition, the cerebral perfusion was incrementally reduced via embolization with microspheres, the color of fluorescent microspheres was changed, and the injection and acquisition processes were repeated (Figure 1). After a total of five to eight fluorescent microsphere colors had been used, the animal was euthanized, and four to six tissue samples (about 10grams each) were surgically excised from the brain (see Table 1). All tissue and blood samples were then analyzed independently (IMT Laboratories) and the resulting perfusion measurements were used as the reference standard[14, 15].

CT Imaging Protocol:

Immediately following each fluorescent microsphere injection, iodinated contrast material (1mL/kg, Isovue 370, Bracco Diagnostics) was intravenously administered at a rate of 5 mL/sec, followed by a saline chaser of 0.5mL/kg at 5mL/sec (Empower CTA, Acist Medical Systems). Dynamic CT scanning was then performed with a 320-slice CT scanner (Aquilion One, Canon America Medical Systems) for 30 seconds to capture the entire contrast time attenuation curve during a full inspiratory breath hold. The following scan parameters were

used: tube voltage, 100 kVp; tube current, 200 mA; detector collimation, 320 × 0.5 mm; volume scanning mode; gantry rotation time, 0.35 second; slice thickness, 0.5 mm; field-of-view, 180 mm; voxel raster, 512 × 512; and reconstruction kernel, FC43 brain with Adaptive Iterative Dose Reduction 3D reconstruction. The CT dose index (mGy) and the dose-length product (mGy·cm) were recorded from the dose sheet. Size-specific dose estimates (mGy) were also calculated for each swine using an effective diameter conversion factor[16, 17]. Finally, a 20-minute time delay was employed between repeated CT acquisition to allow for adequate recirculation and redistribution of contrast material within the parenchyma.

Two-volume dynamic CT perfusion technique:

The existing dynamic CT perfusion techniques use a number of small regions of interest in brain tissue and acquire a number of CT images to measure the tissue contrast pass curve and then estimate the blood flow. The proposed first pass dynamic CT perfusion technique models the whole brain as a single lumped-parameter compartment and derives blood flow from the total contrast mass change within the compartment over two time points as the contrast bolus enters the cerebral circulation[18, 19]. Specifically, assuming no contrast mass outflow from the compartment over the measurement period, the average blood flow (***Q_{ave}*, *ml*/*min***) within the entire compartment is equal to the total integrated change in contrast mass within the compartment (***dM_c*, *mg***) over the measurement time interval (Δ***t***, ***s***), normalized by the average incoming contrast material concentration (***C_{in}***, ***mg***/***ml***) estimated from the ascending pharyngeal artery[18–21] (AIF on Figure 2), as shown in Eq.1.

$$Q_{ave} = \frac{1}{c_{in}} \frac{dM_c}{\Delta t} \quad \text{Eq.1}$$

The average perfusion within the compartment (***P_{ave}*, *ml*/*min*/*g*)** can then be derived by normalizing Eq. 1 the total tissue mass of the brain (***M_T*, *gram***), as shown in Eq. 2.

$$P_{ave} = M_T^{-1}\left(C_{in}^{-1} \frac{dM_c}{dt}\right) \quad \text{Eq.2}$$

Moreover, since the average perfusion (***P_{ave}***) is proportional to the rate of contrast material concentration change within the compartment (Δ***HUave***, ***Housefiled unit***), the concentration change for each voxel (Δ***HU***) can be used to derive the absolute perfusion on a voxel-by-voxel basis (***P***, ***ml***/***min***/***g***), as described by Eq 3. Most importantly, given such a theory, only two optimally timed volumes scans, V1 and V2, are mathematically necessary for perfusion measurement, as previously validated in the heart and lung[20]. Specifically, V1 is defined at the base of the arterial time attenuation curve, signifying contrast material entry into the perfusion compartment. V2 is defined at or near the peak of the arterial input function, signifying the time at the maximal rate of contrast mass accumulation[20, 22].

$$P = P_{ave} \frac{\Delta HU}{\Delta HU avc} \quad \text{Eq.3}$$

CT Perfusion Measurement:

For each dynamic CT acquisition series, the volume scans were first registered using deformable registration[23]. A vascular volume-of-interest was defined within the carotid artery using a Vitrea workstation (ViTAL Images; Canon Medical System) and used to generate an arterial time attenuation curve to calculate contrast concentration and to determine V1 and V2 (Figure 2). To avoid partial volume effects within the arterial volume-of-interest, semi-automatic region growing segmentation was performed within the centermost lumen of a segment of the artery (see Table 1) while excluding the peripheral margin of contrast enhancement adjacent to the vessel wall. The enhancement of the voxels within this volume-of-interest were then averaged to yield the true arterial enhancement. The entire brain parenchyma was also segmented into a three-dimensionally volume-of-interest using the Vitrea workstation, , and further used to generate the brain tissue time attenuation curve (Figures 2 and 3). Two-volume scans, V1 and V2, were then systematically selected from each dynamic CT acquisition series where V1 was selected as the first volume scan after external carotid arterial enhancement exceeded 100 HU above baseline blood HU while V2 was selected at the peak of arterial enhancement (Figure 2). Using the previously generated brain tissue volume-of-interest, the whole-brain perfusion was computed as described in Eq. 3. Finally, for regional perfusion measurement, each segmentation of the brain was divided into four to six digital segments using the Vitrea workstation, corresponding to the previously harvested reference fluorescent microsphere tissue samples. Of note, anatomical landmarks and measuring tools were used to ensure correspondence between the digital and physical tissue segments. The average CT perfusion measurements within each digital segment were then quantitatively compared to the corresponding reference standard fluorescent microsphere perfusion measurements.

Statistical Approach:

The CT perfusion measurements from each brain segment were quantitatively compared to the corresponding reference standard fluorescent microsphere perfusion measurements using independent t-test, linear regression, Pearson’s r, and Bland-Altman analysis. The root-mean-square error was also determined. The performance of CT perfusion-based detection of cerebral infarction was calculated by using a cerebral blood flow threshold of 0.126 mL/min/g, which was determined in a prior CT perfusion study of cerebral infarction in a swine model[24]. Sensitivity, specificity, positive and negative predictive values, and area under the receiver operator characteristic curve (AUC) were computed. Statistical software (SPSS, version 22, IBM) was used.

Results:

General:

The mean weight, heart rate, and arterial pressure of the five swine were 55 ±24 kg, 71.0 ±26.1 bpm, and 60.2 ±19.2 mmHg, respectively. An average of 47 dynamic contrast-enhanced volume scans were obtained over each 30 second acquisition. One acquisition for one of the animals was excluded from the dataset due to a power injector error. A total of 33 acquisitions were obtained from the five animals. As four to six regional CT perfusion measurements were calculated from each acquisition, a total of 164 CT perfusion

measurements were compared to the corresponding reference fluorescent microsphere perfusion measurements.

Accuracy and Precision:

For all the brain segments combined, the mean CT perfusion was 0.228 ml/min/g while the mean perfusion by reference fluorescent microsphere was 0.208 ml/min/g (p-value >0.05), as shown in Table 2. Individual mean comparisons from each animal are also shown in Table 2, while regional mean comparisons are summarized in Table 3. CT perfusion measurements showed excellent correlation to corresponding reference standard fluorescent microsphere perfusion measurements by P_{CT}= 1.15 P_{MICRO} - 0.01 (r = 0.93; p-value < 0.01; root-mean-square error = 0.084 mL/min/g), as shown in Figure 4a, with corresponding Bland-Altman analysis shown in Figure 4b. The repeatability of the technique was also evaluated by comparing two CT perfusion measurements under the same degree of embolization and hemodynamic status, where the first (P_{CT1}) and second (P_{CT2}) perfusion measurements were related by P_{CT2} = 0.94P_{CT1} - 0.003 (r = 0.97, p =0.03), as shown in Figure 5a, with corresponding Bland-Altman analysis shown in Figure 5b. Of note, the observed variations of cerebral blood flow amongst different animals is due to differences in degree of embolization and hemodynamic status. By using the previously reported cerebral blood flow threshold of 0.126 mL/min/g in a swine model[24], for CT perfusion-based detection of cerebral infarct, AUC was 0.99 and the diagnostic sensitivity, specificity, and positive and negative predictive values were 91.2%, 95% CI[84,98], 91.7%, 95% CI[86,97], 88.6% 95% CI[81,96], and 93.6%, 95% CI[89,99] respectively, AUC 0.99.

Radiation Dose:

The mean CT dose $index_{vol16}$ and dose-length product of two-volume CT perfusion measurement were estimated to be 25.6 mGy and 410.3 mGy, respectively.

Discussion:

Indication of Results:

This study used a swine model with incremental embolization of the cerebral capillaries to validate the accuracy of a new dynamic CT perfusion technique for absolute cerebral blood flow measurement. Specifically, the regional and global perfusion measurement with the CT perfusion technique demonstrated a high level of agreement with corresponding reference fluorescent microsphere perfusion measurement, as indicated by t-testing and regression analysis (Tables 2 and 3, Figure 4). Moreover, by extrapolating a previously reported cerebral blood flow threshold of 0.126 mL/min/g in a swine model[24], our CT perfusion-based technique showed excellent theoretical detection of cerebral infarct with an AUC of 0.99. The results of this study indicate that the CT perfusion technique can accurately measure absolute brain perfusion using only two volume scans, i.e., there is significant potential for radiation dose reduction in dynamic CT perfusion of the brain, although further prospective validation studies of the two-volume CT perfusion technique are necessary.

Comparison to Previous Studies:

Our results are consistent with previous cardiac and lung perfusion studies which validated the same two-volume, dynamic CT perfusion technique for accurate myocardial and lung perfusion measurement[20, 21, 25–28]. Furthermore, recent studies show accurate absolute cerebral blood flow measurement in a focal ischemic stroke swine animal model with dynamic CT as compared to MRI, PET, and histology[3, 24]. One of these studies determined that the cerebral blood flow threshold obtained with dynamic CT perfusion measurement is as effective as diffusion-weighted imaging in delineation of the acute infarct core[3]. Nevertheless, other studies found considerable variation in both the accuracy of perfusion measurement and the cutoff thresholds used by conventional dynamic CT perfusion algorithms to determine the infarction core and ischemic penumbra of stroke patients[29–32]. Specifically, the maximum slope model and deconvolution model rely on attenuation changes in small tissue volumes of interest over many consecutive acquisitions for reliable blood flow measurement, at the cost of high radiation dose. Combined with the rapid transit and exit of contrast material from these volumes of interest over the measurement duration, perfusion measurements are known to produce considerable variation[6, 7]. Hence, many current techniques employ relative perfusion rather than absolute perfusion for comparison of ipsilateral ischemia to contralateral normal perfusion but lose relevant flow information as a result.

Novelty of the Present Work:

The two-volume CT perfusion technique was developed to address the above limitations. First, the recent advances in CT technology with improved temporal resolution has made it to image the whole brain in less than 2 seconds[33]. Thus, the two-volume CT perfusion technique can model the entire brain as a single lumped-parameter perfusion compartment. Given the large volume of the compartment, the transit time between contrast entry and exit is significantly increased; hence, CT perfusion measurements can be made before contrast material exits the compartment, resulting in improved accuracy[19, 20, 25, 35]. This has the potential to improve absolute regional brain perfusion quantification to determine core infarct versus ischemic penumbra, which is of great importance when stratifying stroke patients for invasive endovascular reperfusion[36]. Second, as the total amount of contrast accumulating within the compartment is large, higher contrast-to-noise ratio can be obtained as compared with existing CT perfusion techniques using small volumes-of-interest. As a result, the radiation dose associated with dynamic CT perfusion of the brain has the potential to be dramatically reduced by the two-volume CT perfusion technique. Finally, given the timing of the second volume scan at the peak of the arterial time attenuation curve, it may also be used as a co-registered CT angiogram, assuming the tube current is adjusted accordingly. Hence, the two-volume CT perfusion technique has the potential to provide both morphological and physiological information in the same low-dose exam; a one-stop-shop solution to CT-based assessment of ischemic stroke. Nevertheless, true low-dose prospective implementation of the CT perfusion technique combined with CT angiography remains the subject of future work.

Potential for Radiation Dose Reduction:

In this study, only two volume scans were systematically selected for retrospective CT perfusion measurement, simulating a low-dose prospective protocol. Hence, if such a protocol were to be implemented prospectively in human subjects at 100 kVp and 200 mA, the CT dose index of perfusion measurement would be 25.6 mGy, corresponding to an estimated effective radiation dose of 0.86 mSv, with a standard head conversion factor of 0.0021[17] and a 16-cm of craniocaudal coverage. This dose is markedly lower than the average 5 mSv dose of current conventional whole-brain CT perfusion techniques[37]. Further optimizations of tube current, tube potential, and reconstruction parameters should be investigated for further radiation dose reduction.

Limitations:

This study has some limitations. First, the sample size of five swine was small. However, multiple CT perfusion acquisitions were obtained in each animal over a range of brain embolization levels. Additionally, multiple brain segments were assessed for each acquisition in each animal, yielding a large number of measurements to compare with the reference standard fluorescent microsphere perfusion measurements. Second, even though we showed an excellent detection of infarct core by using previously reported cerebral blood flow threshold in swine[24], inducing focal cerebral ischemia or infarction was not feasible with this swine model due to the rete mirabile and rich collateral blood flow in the brain of swine. Hence, future studies should employ focal cerebral infarctions through surgical approaches, i.e., by occluding an intracranial artery or via transcranial injection of potent vasoconstrictors such as endothelin-1[3]. Third, in the current study, the time delay between the two volume scans was estimated using the entire contrast pass curve with multiple volume scans, which is clinically unrealistic for a low-dose technique. Consequently, the clinical implementation of the low-dose technique will use dynamic bolus tracking for acquisition of the first volume scan (V1). The second volume scan (V2) will then be acquired using a timing protocol based on contrast injection time[26]. Nevertheless, true prospective acquisition of a low-dose technique is the subject of future work. Fourth, given that only two volume scans are required by this technique, transit time parameters (e.g. Tmax) cannot be determined with this technique. However, the two-volume technique allows for fast arterial inflow evaluation without venous contamination, which may allow for a more robust determination of absolute regional arterial cerebral blood flow and improved sensitivity to differences in blood flow between brain regions, e.g. infarct core and ischemic tissue.

Summary:

CT perfusion measurements were in good agreement with the reference standard fluorescent microsphere perfusion measurements. Moreover, such measurements were achieved using only two volume scans and a single contrast injection. Hence, accurate assessment of brain perfusion is feasible with the two-volume CT perfusion technique at a low radiation dose, as compared to the existing CT perfusion techniques. As a result, the two-volume CT perfusion technique has the potential to be used for accurate diagnostic assessment, risk stratification, and follow-up of patients with stroke, vasospasm, and intracranial tumors.

References:

1. Benjamin EJ, Virani SS, Callaway CW, Chamberlain AM, Chang AR, Cheng S, et al. Heart disease and stroke statistics-2018 update: A report from the american heart association. Circulation. 2018;137:e67–e492 [PubMed: 29386200]
2. Krishnan P, Murphy A, Aviv RI. Ct-based techniques for brain perfusion. Top Magn Reson Imaging. 2017;26:113–119 [PubMed: 28520657]
3. d'Esterre CD, Aviv RI, Morrison L, Fainardi E, Lee TY. Acute multi-modal neuroimaging in a porcine model of endothelin-1-induced cerebral ischemia: Defining the acute infarct core. Transl Stroke Res. 2015;6:234–241 [PubMed: 25876960]
4. Mir DI, Gupta A, Dunning A, Puchi L, Robinson CL, Epstein HA, et al. Ct perfusion for detection of delayed cerebral ischemia in aneurysmal subarachnoid hemorrhage: A systematic review and meta-analysis. AJNR Am J Neuroradiol. 2014;35:866–871 [PubMed: 24309123]
5. Jain R. Perfusion ct imaging of brain tumors: An overview. AJNR Am J Neuroradiol. 2011;32:1570–1577 [PubMed: 21051510]
6. Kudo K, Sasaki M, Ogasawara K, Terae S, Ehara S, Shirato H. Difference in tracer delay-induced effect among deconvolution algorithms in ct perfusion analysis: Quantitative evaluation with digital phantoms. Radiology. 2009;251:241–249 [PubMed: 19190251]
7. Kudo K, Christensen S, Sasaki M, Ostergaard L, Shirato H, Ogasawara K, et al. Accuracy and reliability assessment of ct and mr perfusion analysis software using a digital phantom. Radiology. 2013;267:201–211 [PubMed: 23220899]
8. American Association of Physicists in Medicine. Routine adult brain perfusion. 2016, March 12
9. Bamberg F, Hinkel R, Schwarz F, Sandner TA, Baloch E, Marcus R, et al. Accuracy of dynamic computed tomography adenosine stress myocardial perfusion imaging in estimating myocardial blood flow at various degrees of coronary artery stenosis using a porcine animal model. Investigative Radiology. 2012;47:71–77 [PubMed: 22178894]
10. Bartoli CR, Okabe K, Akiyama I, Coull B, Godleski JJ. Repeat microsphere delivery for serial measurement of regional blood perfusion in the chronically instrumented, conscious canine. J Surg Res. 2008;145:135–141 [PubMed: 17632127]
11. Gillan LA. Blood supply to brains of ungulates with and without a rete mirabile caroticum. J Comp Neurol. 1974;153:275–290 [PubMed: 4817350]
12. Dondelinger RF, Ghysels MP, Brisbois D, Donkers E, Snaps FR, Saunders J, et al. Relevant radiological anatomy of the pig as a training model in interventional radiology. Eur Radiol. 1998;8:1254–1273 [PubMed: 9724449]
13. Wakhloo AK, Lieber BB, Siekmann R, Eber DJ, Gounis MJ. Acute and chronic swine rete arteriovenous malformation models: Hemodynamics and vascular remodeling. AJNR Am J Neuroradiol. 2005;26:1702–1706 [PubMed: 16091518]
14. Bamberg F, Hinkel R, Schwarz F, Sandner TA, Baloch E, Marcus R, et al. Accuracy of dynamic computed tomography adenosine stress myocardial perfusion imaging in estimating myocardial blood flow at various degrees of coronary artery stenosis using a porcine animal model. Invest Radiol. 2012;47:71–77 [PubMed: 22178894]
15. Bartoli CR, Okabe K, Akiyama I, Coull B, Godleski JJ. Repeat microsphere delivery for serial measurement of regional blood perfusion in the chronically instrumented conscious canine. J Surg Res. 2008;145:135–141 [PubMed: 17632127]
16. Boone J, Strauss K, Cody D, McCollough C, McNitt-Gray M, Toth T, et al. Size-specific dose estimates (ssde) in pediatric and adult body ct examinations: Report of aapm task group 204. College Park, Md: American Association of Physicists in Medicine. 2011
17. Brady SL, Kaufman RA. Investigation of american association of physicists in medicine report 204 size-specific dose estimates for pediatric ct implementation. Radiology. 2012;265:832–840 [PubMed: 23093679]
18. Molloi S, Bednarz G, Tang J, Zhou Y, Mathur T. Absolute volumetric coronary blood flow measurement with digital subtraction angiography. Int J Cardiovasc Imaging. 1998;14:137–145
19. Molloi S, Zhou Y, Kassab GS. Regional volumetric coronary blood flow measurement by digital angiography: In vivo validation. Acad Radiol. 2004;11:757–766 [PubMed: 15217593]

20. Hubbard L, Lipinski J, Ziemer B, Malkasian S, Sadeghi B, Javan H, et al. Comprehensive assessment of coronary artery disease by using first-pass analysis dynamic ct perfusion: Validation in a swine model. Radiology. 2018;286:93–102 [PubMed: 29059038]
21. Ziemer BP, Hubbard L, Lipinski J, Molloi S. Dynamic ct perfusion measurement in a cardiac phantom. Int J Cardiovasc Imaging. 2015;31:1451–1459 [PubMed: 26156231]
22. Zhao Y, Hubbard L, Malkasian S, Abbona P, Molloi S. Dynamic pulmonary ct perfusion using first-pass analysis technique with only two volume scans: Validation in a swine model. Plos One. 2020;15:e0228110 [PubMed: 32049969]
23. Modat M, Ridgway GR, Taylor ZA, Lehmann M, Barnes J, Hawkes DJ, et al. Fast free-form deformation using graphics processing units. Comput Methods Programs Biomed. 2010;98:278–284 [PubMed: 19818524]
24. Wright EA, d'Esterre CD, Morrison LB, Cockburn N, Kovacs M, Lee TY. Absolute cerebral blood flow infarction threshold for 3-hour ischemia time determined with ct perfusion and 18f-ffmz-pet imaging in a porcine model of cerebral ischemia. Plos One. 2016;11:e0158157 [PubMed: 27347877]
25. Hubbard L, Ziemer B, Lipinski J, Sadeghi B, Javan H, Groves EM, et al. Functional assessment of coronary artery disease using whole-heart dynamic computed tomographic perfusion. Circ Cardiovasc Imaging. 2016;9
26. Hubbard L, Malkasian S, Zhao Y, Abbona P, Molloi S. Timing optimization of low-dose first-pass analysis dynamic ct myocardial perfusion measurement: Validation in a swine model. European Radiology Experimental. 2019;3:16 [PubMed: 30945100]
27. Hubbard L, Malkasian S, Zhao Y, Abbona P, Kwon J, Molloi S. Low-radiation-dose stress myocardial perfusion measurement using first-pass analysis dynamic computed tomography: A preliminary investigation in a swine model. Invest Radiol. 2019;54:774–780 [PubMed: 31633574]
28. Zhao Y, Hubbard L, Malkasian S, Abbona P, Molloi S. Dynamic pulmonary ct perfusion using first-pass analysis technique with only two volume scans: Validation in a swine model. Plos One. 2020;(In Press)
29. Bivard A, Levi C, Spratt N, Parsons M. Perfusion ct in acute stroke: A comprehensive analysis of infarct and penumbra. Radiology. 2013;267:543–550 [PubMed: 23264345]
30. Austein F, Riedel C, Kerby T, Meyne J, Binder A, Lindner T, et al. Comparison of perfusion ct software to predict the final infarct volume after thrombectomy. Stroke. 2016;47:2311–2317 [PubMed: 27507864]
31. Kudo K, Sasaki M, Yamada K, Momoshima S, Utsunomiya H, Shirato H, et al. Differences in ct perfusion maps generated by different commercial software: Quantitative analysis by using identical source data of acute stroke patients. Radiology. 2010;254:200–209 [PubMed: 20032153]
32. Koopman MS, Berkhemer OA, Geuskens R, Emmer BJ, van Walderveen MAA, Jenniskens SFM, et al. Comparison of three commonly used ct perfusion software packages in patients with acute ischemic stroke. J Neurointerv Surg. 2019;11:1249–1256 [PubMed: 31203208]
33. Lin L, Bivard A, Krishnamurthy V, Levi CR, Parsons MW. Whole-brain ct perfusion to quantify acute ischemic penumbra and core. Radiology. 2016;279:876–887 [PubMed: 26785041]
34. Page M, Nandurkar D, Crossett MP, Stuckey SL, Lau KP, Kenning N, et al. Comparison of 4 cm z-axis and 16 cm z-axis multidetector ct perfusion. Eur Radiol. 2010;20:1508–1514 [PubMed: 20013273]
35. Molloi S, Bednarz G, Tang J, Zhou Y, Mathur T. Absolute volumetric coronary blood flow measurement with digital subtraction angiography. Int J Cardiovas Imag. 1998;14:137–145
36. Nogueira RG, Jadhav AP, Haussen DC, Bonafe A, Budzik RF, Bhuva P, et al. Thrombectomy 6 to 24 hours after stroke with a mismatch between deficit and infarct. N Engl J Med. 2018;378:11–21 [PubMed: 29129157]
37. Manniesing R, Oei MT, van Ginneken B, Prokop M. Quantitative dose dependency analysis of whole-brain ct perfusion imaging. Radiology. 2016;278:190–197 [PubMed: 26114226]

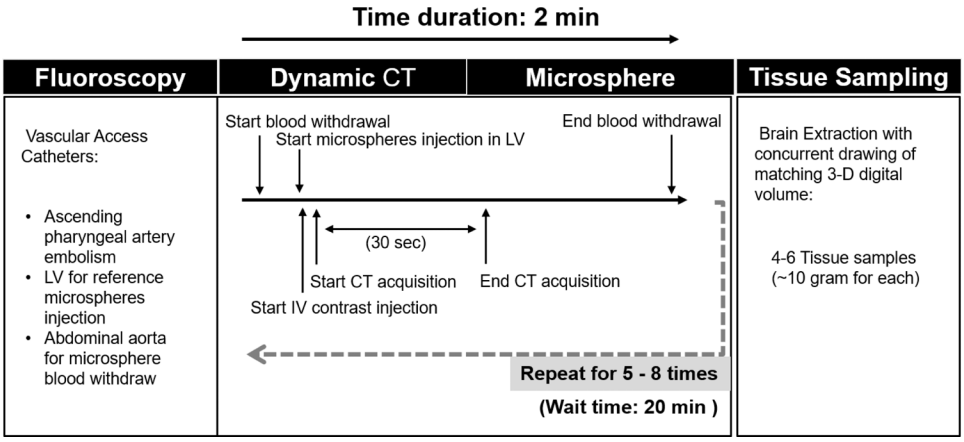

Figure 1.

Flow chart of the experimental design. Blood was withdrawn from the abdominal aorta at a rate of at 10 ml/min for 2 min. IV contrast was injected at a rate of 5 mL/sec. TAC: time attenuation curve. V1 and V2: volumes 1 and 2 used for CT perfusion measurement.

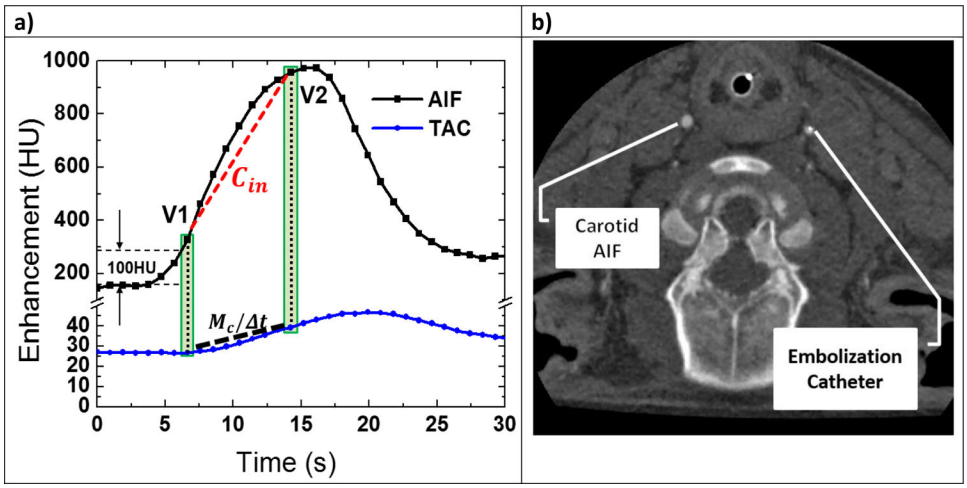

Figure 2.

Two-volume CT perfusion measurement protocol. **a)** Top curve: arterial input function of the external carotid artery (AIF); bottom curve, time attenuation curve(TAC) for the brain parenchyma; HU=Hounsfield Units; $\boldsymbol{C_{in}}$, average input concentration; $\boldsymbol{M_c}$, integrated change in contrast mass; $\Delta \boldsymbol{t}$, measurement time between V1 and V2. b) **b)** CT image showing one carotid artery used for AIF generation and the other corotid used for inducing embolization.

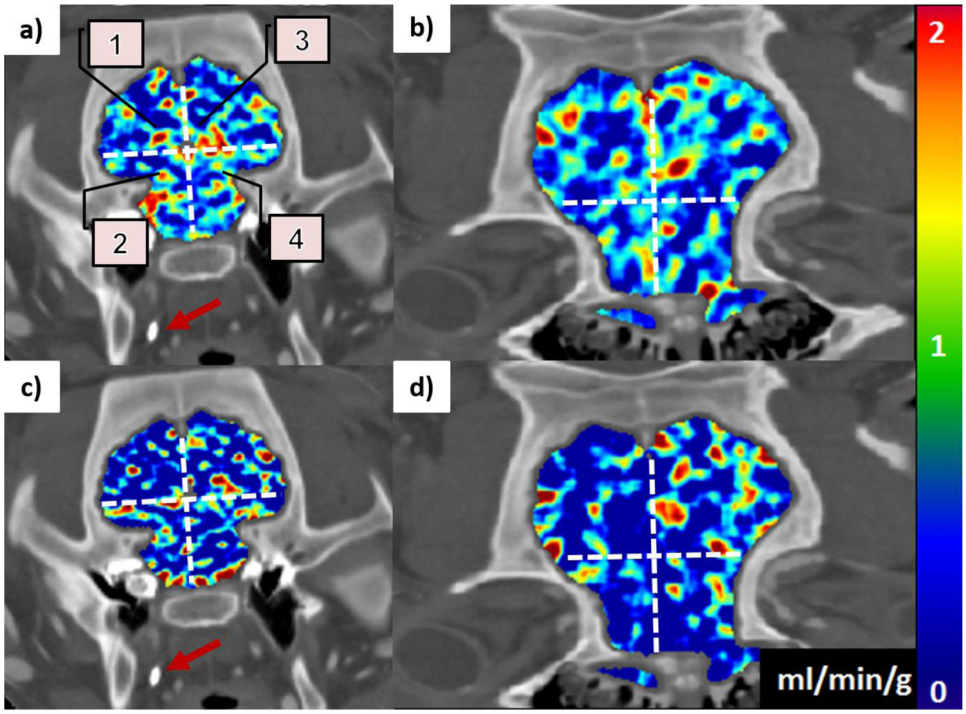

Figure 3.

Perfusion color maps generated by the two-volume CT perfusion technique in axial (a and c) and coronal (b and d) planes. Baseline (a and b) and postembolization maps (c and d) of the same slice are shown. Red arrows indicate embolization catheter within the ascending pharyngeal artery. The color bar indicates quantitative perfusion in ml/min/g. Specifically, four segments were marked for the regional perfusion comparison, including the left posterior and anterior lobes (Segment 1 & 2) and the right posterior and anterior lobes (Segment 3 & 4), with baseline reference fluorescence microsphere perfusions of 0.48, 0.55, 0.47, and 0.48 ml/min/g and the postembolization perfusions of 0.15, 0.16, 0.14 and 0.12 ml/min/g, respectively.

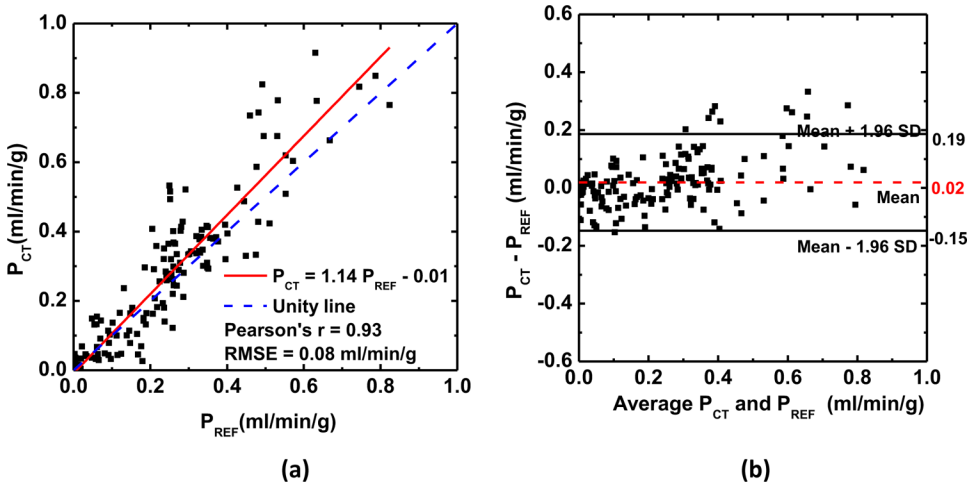

Figure 4.

Regression comparing the result of low-dose CT perfusion measurement to the reference standard microsphere perfusion measurement (P_{CT} and P_{REF}, respectively) (a), with corresponding Bland-Altman analysis shown (b). RMSE indicates root-mean-square-error.

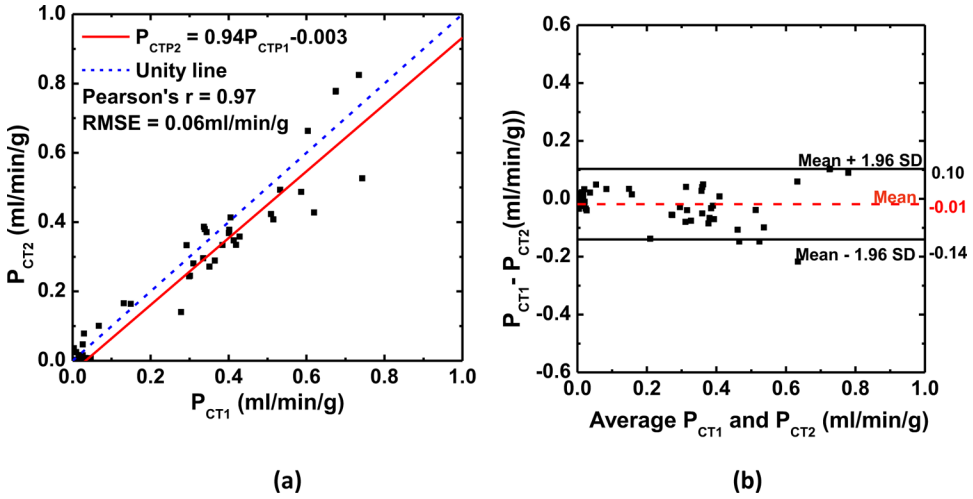

Figure 5:

Regression and Bland-Altman analyses comparing the two repeatable CT perfusion measurements ($P_{CT1}$and P_{CT2}, respectively) (a), with corresponding Bland-Altman analysis shown (b). RMSE indicates root-mean-square-error.

Table 1.

General experimental details for each animal study.

Animal number	Animal weight (kg)	Total brain mass (g)	Average tissue sample mass (g)	Diameter of AIF (mm)	Length of AIF (mm)
1	35.0	88.68	10.23±0.22	4.5	36.1
2	34.0	84.23	9.78±0.10	4.7	34.0
3	45.5	55.34	9.38±0.54	4.3	44.9
4	63.5	84.70	8.99±0.51	5.2	50.4
5	65.0	98.14	9.57±0.26	5.1	46.9

Note.— Tissue sample mass data expressed as mean ± standard. AIF - indicates arterial input function.

Table 2.

Mean brain CT perfusion as compared with reference microsphere perfusion per animal

Animal Number	Number of Samples (n)	Microsphere Reference Perfusion (ml/min/g)	CT Perfusion (ml/min/g)	P-value ($\alpha < 0.05$)
1	32	0.42 ± 0.22	0.50 ± 0.27	0.22
2	16	0.30 ± 0.04	0.34 ± 0.05	0.05
3	20	0.02 ± 0.04	0.01 ± 0.02	0.27
4	48	0.24 ± 0.11	0.26 ± 0.15	0.46
5	48	0.08 ± 0.10	0.07 ± 0.11	0.65
All	168	0.21 ± 0.19	0.23 ± 0.23	0.39

Note.— Perfusion data expressed as mean ± standard. P-value less 0.05 indicates significant difference.

Table 3.

Mean brain CT perfusion as compared with reference microsphere perfusion per brain segment for all animals combined.

Brain Segment	Number of Samples (n)	Microsphere Reference Perfusion (ml/min/g)	CT Perfusion (ml/min/g)	P-value (α < 0.05)
Right Hemisphere	84	0.21 ± 0.19	0.22 ± 0.22	0.75
Anterior	34	0.22 ± 0.21	0.25 ± 0.23	0.19
Middle	16	0.16 ± 0.13	0.15 ± 0.13	0.71
Posterior	34	0.23 ± 0.19	0.23 ± 0.24	0.90
Left Hemisphere	84	0.21 ± 0.18	0.24 ± 0.24	0.38
Anterior	34	0.22 ± 0.21	0.24 ± 0.25	0.74
Middle	16	0.17 ± 0.14	0.18 ± 0.17	0.86
Posterior	34	0.21 ± 0.18	0.26 ± 0.26	0.37

Note.— Perfusion data expressed as mean ± standard. P-value less 0.05 indicates significant difference.